Wu S, Zhu W, Peng Y, Wang L, Hong Y, Huang L, Dong D, Xie J, Merchen T, Kruse E, Guo ZS, Bartlett D, Fu N, He Y.

The Antitumor Effects of Vaccine-Activated CD8$^+$ T Cells Associate with Weak TCR Signaling and Induction of Stem-Like Memory T Cells.

***Cancer Immunology Research* 2017, 5(10), 908-919**

DOI link to article:

https://doi.org/10.1158/2326-6066.CIR-17-0016

Date deposited:

17/11/2017

Embargo release date:

29 August 2018

The antitumor effects of vaccine-activated CD8$^+$ T cells associate with weak TCR signaling and induction of stem-like memory T cells

Sha Wu[1,4,*], Wei Zhu[1,5,*], Yibing Peng[1], Lan Wang[1], Yuan Hong[1], Lei Huang[1,ǂ], Dayong Dong[1], Junping Xie[1], Todd Merchen[1,3], Edward Kruse[1,3], Zong Sheng Guo[6], David Bartlett[6], Ning Fu[5], and Yukai He[1,2]

[1]Georgia Cancer Center, [2]Department of Medicine, and [3]Department of Surgery, Medical College of Georgia, Augusta University, Augusta, GA

[4]Department of Immunology, [5]Division of Laboratory Medicine of Zhujiang Hospital, Southern Medical University, Guangzhou, China

[6]University of Pittsburgh Cancer Institute, Pittsburgh, PA

ǂ Current address: Institute of Cellular Medicine, Newcastle University Medical School, Newcastle, UK

[*]Co-first authors

Correspondences: Yukai He, Georgia Cancer Center, Medical College of Georgia, Augusta University, Augusta, GA 30912. Phone: 706-721-2728; Email: yhe@augusta.edu. Ning Fu, Division of Laboratory Medicine of Zhujiang Hospital, Southern Medical University, Guangzhou, China; Phone: 86-20-61647440; email: zfzn2013@126.com.

Running title: Antitumor effects associate with weak TCR signaling and Tscm

Keywords: Stem-like memory T cells, Cancer Vaccine, TCR downregulation, TCR signaling strength, alpha fetoprotein

Funding: This work is funded by NCI 1R01CA168912 and Georgia Cancer Center Grant to Dr. He.

Abstract

To understand why vaccine-activated tumor-specific T cells often fail to generate antitumor effects, we studied two α-fetoprotein–specific $CD8^+$ T cells (Tet_{499} and Tet_{212}) that had different antitumor effects. We found that Tet_{499} required high antigen doses for re-activation, but could survive persistent antigen stimulation and maintain their effector functions. In contrast, Tet_{212} had a low threshold of re-activation, but underwent exhaustion and apoptosis in the presence of persistent antigen. *In vivo*, Tet_{499} cells expanded more than Tet_{212} upon re-encountering antigen and generated stronger antitumor effects. The different antigen responsiveness and antitumor effects of Tet_{212} and Tet_{499} cells correlated with their activation and differentiation states. Compared to Tet_{212}, the population of Tet_{499} cells was less activated and contained more stem-like memory T cells (Tscm) that could undergo expansion *in vivo*. The TCR signaling strength on Tet_{499} was weaker than Tet_{212}, correlating with more severe Tet_{499} TCR downregulation. Weak TCR signaling may halt T-cell differentiation at the Tscm stage during immune priming and also explains why Tet_{499} re-activation requires a high antigen dose. Weak TCR signaling of Tet_{499} cells in the effector stage will also protect them from exhaustion and apoptosis when they re-encounter persistent antigen in tumor lesion, which generates antitumor effects. Further investigation of TCR downregulation and manipulation of TCR signaling strength may help design cancer vaccines to elicit a mix of tumor-specific $CD8^+$ T cells, including Tscm, capable of surviving antigen re-stimulation to generate antitumor effects.

Introduction

The success of using checkpoint blockade to unleash antitumor immunity (1) confirms that activation of the immune system can control cancer growth. Intensive efforts by vaccine researchers have yielded a variety of immunization approaches that can elicit tumor-specific immunity (2). Despite induction of tumor-specific T cells, however, the antitumor effect of cancer vaccines remains disappointing (3). Evidence from both animal models (4,5) and human trials (6) suggests that the presence of tumor antigen–specific T cells does not necessarily translate into antitumor effects. The limited antitumor effect of tumor-specific T cells has been attributed to immune suppression (7) as well as to T-effector cell (Teff) exhaustion (8,9). However, the lack of correlation between the frequency of antigen-specific T cells and antitumor effects (10-12) also suggests that intrinsic cell attributes may play a role in determining their antitumor outcome (13). Although high "functional avidity" of antigen-specific T cells might be a measure of antitumor efficacy (14-16), contrasting evidence shows that high avidity T cells are associated with weaker antitumor effects (17,18). Indeed, in chronic infections (19,20), the competitiveness of high-avidity T cells comes at a cost, i.e., over-activation, exhaustion, and apoptosis of Teff cells in the presence of persistent antigen stimulation, a scenario that also exists in tumor lesions. Thus, the attributes of $CD8^+$ T cells and mechanisms underpinning the antitumor efficacy of tumor-specific immunity remain unclear and require in-depth investigation in order to improve the efficacy of current immunotherapies.

Lentivector (lv) activates $CD8^+$ T-cell responses (21,22) because of its transduction of dendritic cells (23). We found that immunization with lv-expressing epitope-optimized α-fetoprotein (opt-AFP) activated $CD8^+$ cells to prevent carcinogen-induced autochthonous hepatocellular carcinoma (HCC) in mice (24). But it is not clear whether different epitope-specific $CD8^+$ cells all have antitumor effect. In the current study, we investigated the antitumor effects of two AFP epitope-specific $CD8^+$ cells that could be reproducibly induced by lv immunization. We found that epitope AFP_{212}- and AFP_{499}- specific $CD8^+$ cells (hereafter as Tet_{212} and Tet_{499}) generated different antitumor effects. We thus studied the molecular and cellular attributes of vaccine-activated T cells that are associated with their antitumor effects. We found

that Tet_{499} were insensitive to antigen stimulation and survived persistent *in vitro* antigen re-stimulation and maintained their effector functions. In contrast, Tet_{212} were sensitive to antigen re-stimulation, resulting in more expansion at low doses of antigen, but became exhausted and apoptotic in the presence of high and persistent antigen. *In vivo,* Tet_{499} generated more expansion than Tet_{212} upon re-encountering antigen. The different antigen responsiveness of Tet_{212} and Tet_{499} cells correlated to their different TCR signaling strength and the presence of stem-like memory T cells (Tscm), which had robust *in vivo* expansion. The TCR signaling on Tet_{499} was weaker, associated with severe TCR downregulation. Thus, TCR downregulation and weakened TCR signaling likely prevent Tet_{499} from over-activation and enhances Tscm responses in the priming phase, but also protect Teff from exhaustion and apoptosis at effector phase. Our data suggest that further investigation into the molecular mechanisms of how to control TCR downregulation and TCR signaling strength may help design cancer vaccines to elicit a diverse and healthy mix of tumor-specific $CD8^+$ T cells, especially Tscm, to generate antitumor effects.

Materials and Methods

Mice

C57BL/6 (CD45.2 and CD45.1) and C3H mice were from Charles River. Nur77^{GFP} mice (25) were from Jackson Laboratory. Mice were bred and maintained in specific pathogen-free facility at Augusta University. Animal protocols were approved by the Institutional Animal Care and Use Committee.

Tetramers

The PE-labeled H-2D^b/AFP$_{212}$ and PE- or APC- labeled H-2K^b-D^b/AFP$_{499}$ tetramers were prepared by NIH Tetramer Core Facility. In the H-2K^b-D^b/AFP499 Tetramer, the α3 domain of H-2K^b is replaced with α3 domain of H-2D^b to reduce non-specific binding. The AFP$_{212}$ and AFP$_{499}$ peptides bind to H-2D^b and H-2K^b, respectively. Wild-type AFP peptides were used to prepare tetramers.

Cell lines, tumor challenge and tumor induction

EL4 and 293T cells were purchased from ATCC (Manassas, VA) in 2010. Cells received from ATCC were immediately expanded and stored in liquid nitrogen. Each time, one vial of cells were thawed and used for less than 6 passages to maintain their authenticity. EL4-AFP tumor cells were established previously (24) by transducing parental EL4 cells with lv expressing mouse AFP. Cell lines were checked for mycoplasma by PCR test (Fisher Scientific). For tumor challenge, 1X10^5 EL4-AFP cells were injected subcutaneously into the flank of C57BL/6 mice. The induction of autochthonous HCC with diethylnitrosamine (DEN) (Sigma) was conducted as described (24). Briefly, 2wks old of the F1 mice of B6XC3H cross-bred was intraperitoneally injected with 50μg of DEN per gram of mouse weight.

Recombinant viral vectors and immunization

The plasmid expressing epitope-optimized mouse AFP (opt-AFP) was described (24). The shorter AFP fragments of AFP142 and AFP164 were cloned into pLenti6 (Invitrogen) by PCR cloning. The lvs were prepared by transient co-transfection of 293T cells and the vectors were concentrated and titered by measuring the p24 level as described (21).

To construct recombinant vv expressing the opt-AFP, a shuttle plasmid vector pG10 was used (26). The opt-AFP gene was cloned into the vector behind the p7.5 early gene promoter to create pG10-opt-AFP. CV-1 cells in 6-well plates were infected with a wild-type vaccinia virus of WR strain at multiplicity of infection of 0.1, and then transfected with pG10-opt-AFP by SuperFect reagent (Qiagen). The recombinant vv was selected in human TK-143 cells with addition of BrdU in the medium. After three rounds of plaque purification, the purity of the virus was verified by PCR assays for presence of the transgene and deletion of the viral thymidine kinase gene, and by fluorescence of DsRED in the infected cells. The virus, designated as opt-AFP-vv, was amplified in HeLa cells and purified by a standard procedure (26).

For immunization, $2X10^7$ transduction units of opt-AFP-lv were injected via footpad. To boost immune responses, $1.5\ X10^7$ infectious units of recombinant opt-AFP-vv were injected intraperitoneally. For immunization in the autochthonous HCC model, 2 months old F1 mice of B6XC3H that had been induced by carcinogen DEN were immunized with opt-AFP-lv and then boosted with opt-AFP-vv at 3 months old.

***In vitro* re-stimulation**

The splenocytes (6 millions) were re-stimulated for the indicated time with various concentration of wild type AFP_{212} (GSMLNEHVC) or AFP_{499} (SSYSNRRL) peptide in the presence of 20IU/ml IL-2 (ProSpec-Tany Technogene). The wild type AFP peptides were used to make sure that the re-stimulated T cells would recognize and kill tumor cells expressing wild type AFP. In some experiments, 10ng/ml of

IL-7 and IL-15 were also added. To maintain peptide level, half of the RPMI medium containing the indicated concentrations of peptides was changed every other day.

In the second setting, the splenic CD8 T cells were purified by magnetic beads from immunized CD45.2 mice. The splenocytes of naïve CD45.1 congenic mice were pulsed with indicated concentrations of AFP_{212} or AFP_{499} peotides for 2hrs. Free peptides were washed away. Two millions of the purified CD8 T cells were then re-stimulated with four millions of peptide-loaded CD45.1 splenocytes in a 24 well plate in RPMI media containing 20IU/ml IL-2. After forty-eight hours, four millions of peptide-loaded CD45.1 fresh splenocytes were added to continue stimulation for another 2 days before analysis.

Immunological staining and flow cytometry analysis

Peripheral mouse blood cells and the splenocytes (fresh or stimulated) were stained with indicated combinations of antibodies plus H-$2D^b$/AFP_{212} or H-$2K^b$-D^b/AFP_{499} tetramers. For tetramer staining after re-stimulation with peptide in the media, the stimulated cells need 12 hours rest to recover the TCR. DAPI was added to exclude dead cells. Intracellular staining of IFNγ was conducted as described (24) after the cells were re-stimulated with peptides in the presence of GolgiStop for 3.5 hours. Events were collected on the LSR II and the data was analyzed using FCS Express III software. The antibodies used in this study include antibodies to mouse CD8 (Clone: 53-6.7, Biolegend), CD45.1 (Clone: A20, Biolegend), CD45.2 (Clone: 104, BD Bioscience), CD44 (Clone: 1M7, Biolegend), CD62L (Clone: MEL-14, Biolegend), CD127 (IL-7Ra) (Clone: A7R34, Biolegend), PD-1 (Clone: 29F.1A12, Biolegend), CCR7 (Clone: 4B12, Biolegend), CD122 (IL-2Rβ) (Clone: TM-β1, Biolegend), Sca-1 (Clone: D7, Biolegend,), CD95 (Clone: SA367H8, Biolegend), IFN-γ (Clone: XMG1.2, Biolegend), Bcl-2 (Clone: BCL/10C4, Biolegend), H-2^K b/H-$2D^b$ (Clone: 28-8-6, Biolegend), TCRβ (Clone: H57-597, BD Bioscience). The Annexin-V and DAPI (4,6-diamidino-2 phenylinole dilactate) were from Biolegend.

CTL assay

The *in vitro* CTL assay was performed as previous described (21,24). The splenocytes from immunized mice were re-stimulated with 2μg/ml of AFP_{212} or AFP_{499} peptide for indicated times in the RPMI media containing 20 units/ml of IL-2. The EL4 and EL4-AFP tumor cells were labeled with 1μM and 0.03μM of 5-(and 6)-Carboxyfluorescein diacetate succinimidyl ester (CFSE) (Invitrogen), respectively, for 10min at 37°C. After washing, equal numbers ($5X10^4$) of $CFSE^{lo}$-labeled target EL4-AFP cells and $CFSE^{hi}$-labeled EL4 control cells were co-cultured in triplicate with the *in vitro* peptide-stimulated splenocytes at the indicated E/T ratios for 6 hours. The killing of target EL4-AFP cells was analyzed by flow cytometry. The specific killing activity was calculated using the formula [1-(ratio of $CFSE^{hi}/CFSE^{lo}$ in the absence of CTL) / (ratio of $CFSE^{hi}/CFSE^{lo}$ in the presence of CTL)] X100 as previously described (21).

Cell Sorting and Adaptive cell transfer

The splenic CD8 T cells were enriched by magnetic beads (Stemcell Technologies) then stained with anti-CD8, CD44, CD62L antibodies plus H-$2D^b$/$mAFP_{212}$ or H-$2K^b$-D^b/mAFP499 tetramer. The tetramer+ cells and their subsets were sorted on FACSAria (BD Biosciences). The sorted cells of indicated number were injected into CD45.1 congenic mice, which were then immunized with opt-AFP-lv. The $CD45.2^+CD8^+Tet^+$ cells in the peripheral blood of CD45.1 mice were monitored once a week by tetramer staining.

Tetramer binding and dissociation assay

The tetramer binding and dissociation assays were conducted as described (27). For tetramer binding assay, one million splenocytes of the immunized mice were stained with anti-CD8 antibody and the indicated concentrations of H-$2D^b$/AFP_{212} or H-$2K^b$-D^b/AFP_{499} tetramer. Between the tetramer concentrations of 6.5μg/ml to 13μg/ml, the percent of Tet_{212} and Tet_{499} cells did not increase further, suggesting that all the tetramer+ cells were stained. The Tet_{212} and Tet_{499} cells detected at lower tetramer

concentration were compared to those detected at the concentration of 13μg/ml, which was considered as 100%.

For tetramer dissociation assay, the cells were stained with 6.5μg/ml of tetramer. After washing away the free tetramers, the cells were left at room temperature for the indicated times in the presence of anti-H-2K^{b}/H-2D^{b} antibody before they were analyzed for the percent and MFI of the Tet+ cells.

Statistical analysis

Statistical analyses were performed using *T*-test or ANOVA (GraphPad Inc).

Results

Tet_{212} and Tet_{499} have different CTL activity and *in vivo* antitumor effects

To study whether different AFP epitope-specific $CD8^+$ T cells could kill AFP^+ tumor cells, we re-stimulated the splenocytes with AFP_{212} and AFP_{499} peptide in media and used them as effectors for *in vitro* CTL assays (Fig. 1A). After 6-day re-stimulation, splenocytes of naïve and wild-type-AFP-lv immunized mice showed no CTL activity (Fig.1B), consistent with our recent report (24). On the other hand, splenocytes from the opt-AFP-lv immunized mice had CTL activity after AFP_{499} peptide re-stimulation (Fig. 1B and Supplementary Fig. S1A-B). However, after AFP_{212} peptide re-stimulation, splenocytes of the opt-AFP-lv immunized mice generated no CTL activity. Kinetic study demonstrated that the CTL activity of opt-AFP-lv immunized splenocytes was diminished with AFP_{212} peptide, but was enhanced with AFP_{499} peptide, re-stimulation (Supplementary Fig. S1C).

To study whether Tet_{212} and Tet_{499} generated different antitumor effects *in vivo,* we constructed two lvs, AFP142-lv and AFP164-lv, to activate Tet_{212} and Tet_{499} separately (Fig. 1C). We found that, like opt-AFP-lv, AFP164-lv immunization protected mice from AFP^+ tumor challenge. In contrast, all mice immunized with AFP142-lv developed tumors (Fig. 1D). The lack of antitumor effect by Tet_{212} was not due to its incapability of recognizing AFP^+ tumor cells since both Tet_{212} and Tet_{499} cells produced IFNγ after co-culture with EL4-AFP cells (Supplementary Fig. S1D). Together, these data suggest that Tet_{212} and Tet_{499} cells have different responses to tumor antigen *in vitro* and *in vivo*, resulting in different antitumor effects.

Tet_{212} cells differ from Tet_{499} in re-activation threshold, exhaustion and apoptosis

To investigate why Tet_{212} and Tet_{499} generate such different CTL activities and antitumor effects, we studied their antigen responsiveness *in vitro*. To generate more Tet_{212} and Tet_{499} cells, we boosted the lv-immunized mice with vv. The purified $CD8^+$ cells from immunized CD45.2 mice were re-stimulated

with naive CD45.1 splenocytes pulsed with different peptides. After 4-days, we observed a dose-dependent increase of Tet_{212} cells between the pulsed peptide ranges of 0.1-2μg/ml (Fig. 2A). However, at 10μg/ml of AFP_{212} peptide, the percent of Tet_{212} among total CD45.2 $CD8^+$ cells began to decline. Furthermore, re-stimulation with 2μg/ml of AFP_{212} peptide in media reduced Tet_{212} to ~1% (Fig. 2A). In contrast, the percent of Tet_{499} increased only slightly between the pulsed AFP_{499} peptide ranges of 0.1-10μg/ml, and increased more so after re-stimulation with AFP_{499} peptide in media (Fig. 2A). In addition, we analyzed the PD1 and Annexin-V level on Tet_{212} and Tet_{499} after stimulation. We found that, compared to Tet_{499}, the percent of $PD1^+$ Tet_{212} and the MFI of PD1 on Tet_{212} was higher at every dose point (Fig. 2B). Similarly, the percent and MFI of Annexin-V were also higher on Tet_{212} (Fig. 2C). The production of cytokine IFNγ by Tet_{212} cells was inversely related to AFP_{212} peptide dose (Fig. 2D-E). In contrast, the percent and MFI of $IFN\gamma^+$ Tet_{499} cells were directly related to the dose of AFP_{499} peptide.

The exhaustion and apoptosis of Tet_{212} and Tet_{499} cells were also studied when peptides were added directly to the re-stimulation media (Supplementary Fig. S2A). The data showed ~10% of Tet_{212} and Tet_{499} cells being apoptotic prior to re-stimulation. AFP_{212} peptide re-stimulation caused Tet_{212} undergo dose-dependent apoptosis, ~70% of Tet_{212} cell being apoptotic with 2μg/ml of peptide stimulation (Supplementary Fig. S2B-C). In contrast, only ~17% of Tet_{499} cells were apoptotic after AFP_{499} peptide re-stimulation. Consistent with the data, only 5% of Tet_{212} cells, but 80% of Tet_{499} cells, survived 4 day peptide re-stimulation (Supplementary Fig. S2D). Again, more Tet_{212} expressed higher level of PD1 in a dose-dependent manner (Supplementary Fig. S2E). Furthermore, Tet_{212} lost their cytokine production and CTL activity after re-stimulation (Supplementary Fig. S2F). In contrast, the majority of Tet_{499} was not exhausted and maintained their effector function. The exhaustion and apoptosis were different from activation-induced anergy (28) as it could not be rescued by the addition of IL2 or even IL7 and IL15.

In summary, Tet_{212} have a low threshold of re-activation and can be expanded by low dose antigen. But its high sensitivity to antigen re-stimulation leads to progressive upregulation of PD1 and reciprocal

decrease of IFNγ and apoptosis with increasing dose of antigen. In contrast, Tet_{499} have a high re-activation threshold and thus is difficult to activate and expand. But the Tet_{499}'s insensitivity to antigen also protects them from exhaustion and activation-induced apoptosis. As a result, persistent antigen re-stimulation (such as peptide in media) decreased Tet_{212} but increased Tet_{499} cells.

Tet_{499} proliferate better *in vivo* than Tet_{212} in response to emerging tumor antigen.

We then studied *in vivo* re-expansion of Tet_{212} and Tet_{499} upon re-encountering antigen. Tet_{212} and Tet_{499} cells were sorted from immunized CD45.2 mice and transferred into CD45.1 congenic mice followed by immunization (Fig. 3A). The data showed a significant more increase of Tet_{499} than Tet_{212} cells in the CD45.1 mice (Fig. 3B). In addition, the carcinogen-induced autochthonous HCC model was utilized to study *in vivo* antigen responsiveness of Tet_{212} and Tet_{499} cells to emerging AFP tumor antigen (Fig. 3C). We first found that the magnitude of Tet_{499} responses after vv boost was greater than that of Tet_{212} (Fig. 3D), suggesting Tet_{499} cells primed by lv underwent more extensive expansion when re-encountering antigen expressed from vv. Tet_{499} cells were also able to detect emerging AFP antigen in autochthonous HCC and responded by expansion (the spike of Tet_{499} at day 140 in Fig. 3D). In contrast, Tet_{212} cells did not generate expansion by vv boost and could not generate productive response to emerging AFP antigen.

Tet_{499} contain more Tscm, Tcm, and express more antiapoptotic Bcl-2 than Tet_{212}.

We next studied the possible mechanisms underpinning the different antigen responsiveness of Tet_{212} and Tet_{499} cells. Memory T cells, especially Tscm and Tcm, are critical for generating antitumor effect as they can undergo expansion in response to tumor antigen (29-31). To study if the antigen responsiveness and antitumor effect of Tet_{212} and Tet_{499} cells were related to Tscm and Tcm, we stained Tet_{212} and Tet_{499}

with CD44 and CD62L. As demonstrated in Fig. 4A, the Tet^+ $CD8^+$ cells could be grouped into $CD44^+CD62L^-$ Teff (or effector memory, hereafter referred to as Teff), $CD44^+CD62L^+$ Tcm, and the $CD44^-CD62L^+$ naïve-like Tscm. We found that Tet_{499} contained more Tscm and Tcm than Tet_{212} (Fig. 4A). Even after *in vitro* stimulation, the percent of Tcm and Tscm was still higher among Tet_{499} (Fig. 4B). Further analysis showed that, different from the counterpart of naïve $CD8^+$ T cells, the Tet_{499} Tscm expressed more of stem-like cell markers of ScaI, CD122, and CCR7 (Fig. 4C). To minimize non-specific binding, beads enriched $CD8^+$ T cells were pre-blocked by Fc blocker CD16/CD32 antibody. After taking these measures, we verified that Tet_{499} contained more Tscm than Tet_{212} (Supplementary Fig. S3A). The $CD44^-CD62L^+$ Tscm also expressed higher level of CD95 than naïve $CD8^+$ T cells, another potential marker of Tscm (Supplementary Fig. S3B). The presence of Tscm was then confirmed in the Tet_{499} cells by dual-color tetramer staining (Supplementary Fig. S3C).

The resistance to antigen-induced Tet_{499} apoptosis may be also due to the Bcl-2 molecules (32). Indeed, we found that the Tscm of Tet_{499} expressed the highest level of Bcl-2 compared to Tcm and Teff, nearly to the same level as naïve CD8+ cells (Supplementary Fig. S3D). In addition, Bcl-2 level in the Tcm and Teff of Tet_{499} cells was higher than the counterparts of Tet_{212}, suggesting that even at the Tcm and Teff stages, Tet_{499} cells can better survive antigen-induced cell death.

Tscm undergo more *in vivo* expansion than Tcm and Teff upon re-encountering antigen.

In Fig. 3B, we showed that Tet_{499} cells generated more re-expansion. To determine which subsets of Tet_{499} cells could undergo *in vivo* expansion, we sorted the Teff, Tcm, and Tscm and transferred them into CD45.1 mice (Fig. 5A). Because the number of Tscm and Tcm cells in the Tet_{499}^+ population was too low to be efficiently collected, we sorted the Teff, Tcm, and Tscm based on the total $CD8^+$ cells (see sorting strategy and purity of Tscm, Tcm, and Teff in Supplementary Fig. S4A-B). The number of Tet_{499}^+Tscm, Tet_{499}^+Tcm, and Tet_{499}^+Teff was calculated using the percentage of Tet_{499}^+ in the sorted $CD8^+$ Tscm, Tcm, and Teff population (Supplementary Fig. S4C). Equal numbers (2000) of Tet_{499}^+Tscm,

Tet_{499}^{+}Tcm, and Tet_{499}^{+}Teff was transferred into CD45.1 mice. Teff generated no measurable expansion. In contrast, the $CD45.2^{+}$ $CD8^{+}$ cells were detected in the CD45.1 congenic mice receiving Tscm or Tcm cells (Fig. 5B-C). The percent of $CD45.2^{+}Tet_{499}$ cells in the mice receiving Tscm increased by more than 30 fold, from ~1% to ~35%, whereas the percentage of $CD45.2^{+}Tet_{499}$ cells in the mice receiving Tcm increased only 5 times, from ~1% to ~5% (Supplementary Fig.S4C and Fig.5B-C). This data suggests the Tet_{499}^{+}Tscm undergo more expansion than Tet_{499}^{+}Tcm *in vivo* after re-encountering antigen. In addition, after adoptive transfer of Tscm, three populations of cells, Tscm, Tcm, and Teff, were found in the mice (Fig.5D), suggesting that Tscm could differentiate into Tcm and Teff and maintained self-renewal capability.

The TCR signaling strength is weaker on Tet_{499} than on Tet_{212}.

It is postulated that TCR signaling strength affects antigen-induced T-cell differentiation, including induction of Tscm and Tcm (29,33,34), which have a greater potential of expansion when re-encountering the same antigen (35). To determine the TCR signaling strength of Tet_{212} and Tet_{499} cells, we utilized the $Nur77^{GFP}$ mice (25), in which the TCR signaling strength is reflected by GFP intensity on T cells. We found that, fresh Tet_{212} and Tet_{499} cells from immunized $Nur77^{GFP}$ mice were $GFP^{-/low}$ prior to stimulation (Fig. 6A). After re-stimulation with 2μg/ml peptide in media for 4hrs, all Tet_{212} and ~90% of Tet_{499} cells became GFP^{+}, with a higher GFP level on Tet_{212} cells (Fig. 6A-B). The remaining $GFP^{-/low}$ Tet_{499} after peptide stimulation contained more Tscm and Tcm cells; ~40% of them were Tscm and Tcm. Even in the GFP^{+} population, Tet_{499} contained more Tscm and Tcm than Tet_{212} (Supplementary Fig. S5A-C). Peptide titration study revealed that the % and MFI of GFP^{+} Tet_{212} were higher than Tet_{499} at any concentration (Fig. 6C). For example, at 1ng/ml, 80% of Tet_{212} cells were GFP^{+}, whereas only 20% of Tet_{499} cells were GFP^{+}. These data suggest that TCR signaling on Tet_{499} is weaker than Tet_{212}.

Furthermore, Tet_{212} GFP^+ cells had higher CD44 expression than the Tet_{499} GFP^+ cells (Fig. 6D), indicating that the Tet_{499} cells are in a lower activation state.

The TCR signaling strength of Tet_{212} and Tet_{499} cells was further studied by re-stimulating the purified $CD45.2^+CD8^+$ T cells from immunized $Nur77^{GFP}$ mice with peptide-pulsed CD45.1 splenocytes. We found that, prior to re-stimulation, fresh Tet_{212} of immunized mice express higher basal level GFP than Tet_{499} cells (Fig. 6E). Tet_{212} could become GFP^+ even at low concentration of peptide (Fig. 6F). The Tet_{212} cells re-stimulated by splenocytes pulsed with 0.1μg/ml of AFP_{212} peptide expressed higher level of GFP than Tet_{499} re-stimulated by splenocytes pulsed with 10μg/ml of AFP_{499} peptide, suggesting that Tet_{499} TCR signaling is at least 100 times weaker than Tet_{212} TCR signaling.

Compared to Tet_{212}, Tet_{499} TCRs have higher avidity for MHC/peptide but are more downregulated

The low reactivation threshold and stronger TCR signaling on Tet_{212} cells (Figs. 2 and 6) may be caused by high T cell avidity for cognate MHC/peptide. Thus, we conducted a tetramer binding (Fig. 7A) and dissociation (Fig. 7B) assays, which measure the TCR avidity for MHC/peptide complex. The data showed that approximately 90% of the Tet_{499} cells were stained with a low concentration (0.65μg/ml) of H-$2K^b$-D^b/AFP_{499} tetramer. In contrast, to achieve 90% staining of the Tet_{212} cells, 10 times more (6.5μg/ml) of the H-$2D^b$/AFP_{212} tetramer was required. In addition, the Tet_{499} TCR binding to MHC/peptide was dissociated more slowly (Fig. 7B). Thus, the Tet_{499} TCRs have a higher avidity for MHC/peptide.

Another factor that can influence the TCR signaling strength is the amount of TCR on the cell surface, which is normally downregulated after activation (36). Thus, we examined the TCR levels on Tet_{212} and Tet_{499} cells. The splenocytes from immunized mice were stained with antibodies to CD8, CD44, CD62L, TCR Vβ (Clone 57-597), plus tetramer. The TCR Vβ levels on Tet^+ $CD8^+$ T cells were compared to $Tet^-CD44^-CD62L^+$ naïve $CD8^+$ T cells. Our data demonstrated that TCRs on Tet_{499} were more

downregulated (Fig.7C-E). Tet_{499} had only 40% of the TCRs as naïve $CD8^+$ cells. In contrast, Tet_{212} had ~80% of the TCRs as naïve $CD8^+$ cells. By direct comparison, the Tet_{499} had approximately half the TCRs of Tet_{212} cells (Fig. 7F). The kinetic analysis of TCR downregulation showed that TCR downregulation on Tet_{212} was mild and transient (Fig. 7G). In contrast, TCR downregulation on Tet_{499} was severe and persistent. As the antibody to TCR Vβ staining may be interfered with by tetramers that compete for the same TCR, the CD3 level on Tet_{212} and Tet_{499} cells was thus measured to determine TCR downregulation. The data showed that CD3 was also more downregulated on Tet_{499} than on Tet_{212} (Supplementary Fig. S6A-D). Together, our data showed that, the Tet_{499} TCRs have higher avidity for MHC/peptide, but its level is more downregulated after activation, which may result in ensuing weaker TCR signaling and higher threshold of re-activation.

Discussion

Our findings associate the antitumor effect of vaccine-activated $CD8^+$ T-cells with their antigen sensitivity and activation/differentiation states. First, the antigen sensitivity of two AFP-specific $CD8^+$ T-cells, Tet_{212} and Tet_{499}, is different. Tet_{212} have a lower threshold of re-activation and are sensitive to antigen stimulation, but become exhausted and apoptotic when antigen persists, and generate no antitumor effect *in vivo*. In contrast, Tet_{499} have a higher threshold of re-activation and are more resistant to antigen stimulation, but can survive persistent tumor antigen, maintain their effector function, and generate a potent antitumor effect *in vivo*. Secondly, the vaccine-activated Tet_{212} and Tet_{499} cells are at different differentiation and activation state. Tet_{499} cells are at a lower activation state and consist of diverse subsets at different differentiation stages, including Tscm and Tcm. In contrast, there are no Tscm and few Tcm in Tet_{212}. The Tet_{499} Tscm can undergo extensive *in vivo* expansion when re-encountering antigen. Thirdly, the TCR signaling on Tet_{212} is stronger and associated with mild and transient TCR downregulation. In contrast, the Tet_{499} TCR signaling is weaker, likely due to severe and persistent TCR downregulation.

TCR signaling strength correlates to the activation and magnitude of antigen-specific T cells (37-39). Indeed, data from $Nur77^{GFP}$ mice showed that the TCR signaling on Tet_{212} was stronger, corresponding to a higher magnitude of Tet_{212} response by immunization (24). But, on the other hand, strong TCR signaling can negatively affect the induction of Tscm (29,40). In agreement with this argument, the Tet_{499}, but not Tet_{212} contains Tscm. Stem-like memory immune cells were proposed by Fearon et al (41). The Tscm was found to cause graft vs host disease (35). Gattinoni et al showed that the TCR transgenic gp100-specific Tscm generated *in vitro* by inhibiting Wnt signaling had a better antitumor effect (42). They further found that human Tscm mediated strong antitumor effect in mice bearing human tumors (43). In a retrospective study, Speiser and colleagues found that yellow fever vaccine-induced Tscm in human correlated to long-term protection (44). Here we show that cancer vaccine can elicit Tscm *in vivo*, which

is associated with TCR downregulation and weak TCR signaling, and correlates with stronger antitumor effect.

The engagement of TCR and MHC/peptide and proper TCR signaling are also needed for the re-activation of vaccine-induced T cells to recognize and kill tumor cells. T cells with higher basal level of TCR signaling are more ready for activation (45,46). Even though the Tet_{212} and Tet_{499} activated by vaccine are not naïve cells, their re-activation seems also correlate to their basal TCR signaling. Tet212 have a higher TCR signaling strength and are more ready for re-activation and consequently also suffers from activation induced cell death when antigen persists. In contrast, the Tet_{499} cells with weaker TCR signaling survive persistent antigen stimulation and generate a stronger antitumor effect. This is consistent with previous hypothesis that TCR downregulation may protect T cells from excessive signaling (47). Thus, TCR downregulation and weaker TCR signaling on the activated T cells in the effector phase may protect them from antigen-induced exhaustion and apoptosis, especially in the tumor lesions where the antigen is abundant and the stimulation is likely persistent. But the high concentration of antigens in tumor lesion and the prolonged engagement of T cells and tumor cells will compensate for the lower TCR level and generate sufficient accumulative signaling strength to activate Tet_{499} cells to kill tumor cells.

The association of weak TCR signaling with stronger antitumor effect of T cells seems counter-intuitive. Our finding of Tet_{499} TCR downregulation associated with a strong antitumor effect is also in contrast to a report showing that TCR downregulation limits their efficacy of controlling microbial infection (48). We reason that this is likely due to the difference of antigen level and antigen stimulation duration between microbial infections and tumor lesion. In acute infections, the microbial antigen is transient, and thus T cells with higher level or sensitive TCR should not be exhausted and are more effective to eliminate the infection because of the stronger engagement of TCR and MHC/peptide. On the other hand, in tumor lesion, the T cells are immersed in a pool of tumor antigens for a prolonged period of time, thus T cells with sensitive threshold of re-activation will likely be driven to exhaustion. Only the T cells with weaker TCR signaling may survive persistent antigen stimulation and generate antitumor

effects. In agreement with this theory, in chronic persistent viral infection, T cells are exhausted (49). The report that T cells activated with intermediate affinity peptides (thus intermediate strength of TCR signaling) generate a better antitumor effect (50) is also in agreement with our data.

Based on these findings, we propose a model (Supplementary Fig.S7), in which the TCR signaling strength and the threshold of activation controls the state of T-cell activation, the generation of Tscm, antigen responsiveness, and the antitumor effect of the vaccine-activated $CD8^+$ T cells. In this model, initial high affinity TCR-MHC/peptide complex engagement results in T-cell activation and concurrently generates feedback to downregulate TCR on activated T cells, weakening the TCR signaling to avoid over-activation of T cells in the priming phase. The weakened TCR signaling will allow some activated T cells to halt differentiation at Tscm stage to reserve their potential to generate better responsiveness and stronger antitumor effect when they re-encounter cognate antigen in tumor lesions. Thirdly, the weakened TCR signaling on Teff will protect them from exhaustion and apoptosis upon re-encountering persistent antigen in tumor lesion. In contrast, if the TCR downregulation is mild and transient, TCR signaling will likely drive all activated T cells to become terminal Teff, which not only decrease Tscm, but also predispose the Teff to exhaustion and apoptosis when they re-encounter antigen in tumor lesion.

In this model, we attribute the different TCR signaling strength and antigen sensitivity of Tet_{212} and Tet_{499} cells to their different TCR downregulation. However, these differences may also be due to the inherent difference of internal signaling pathways inside the Tet_{212} and Tet_{499} cells. Whether the high affinity TCR-MHC/peptide engagement also reduces the internal signaling pathway is not clear, nor is the inherent signaling difference between naive Tet_{212} and Tet_{499} cells. Even though our data support that the different antigen responsiveness of vaccine-activated Tet_{212} and Tet_{499} cells relates to their different TCR downregulation and signaling strength, further studies should be done to investigate whether the naïve Tet_{212} and Tet_{499} cells are different in their antigen responsiveness. If naïve Tet_{499} and Tet_{212} cells indeed have inherent signaling difference that is beyond the TCR level, the T cells with higher threshold of activation and capability of resisting antigen-induced cell death may be the ideal host cells for generating

TCR and chimeric antigen receptor (CAR) gene engineered T cells for immunotherapy of solid tumors, where the TCR or CAR gene engineered T cells need to survive persistent antigen stimulation and generate antitumor effect.

This current study also raises questions in cancer vaccines and immunotherapy. The first question is whether TCR signaling strength on any antigen-specific T cells can be manipulated to enhance Tscm generation and to prevent exhaustion in tumor lesion. Secondly, how should cancer vaccine and immunization strategies be devised to find the right balance between eliciting sufficient number of tumor-specific T cells while inducing Tscm to achieve the maximal antitumor effect? Investigation into these questions should help develop more effective cancer vaccines and enhance the antitumor efficacy of current immunotherapies.

Acknowledgement

We acknowledge the stimulating discussion with Dr. Bjoern Peters of La Jolla Institute for Allergy and Immunology and Drs. Rafal Pacholczyk, David Munn, and Esteban Celis at Augusta University. The excellent service of NIH Tetramer Core Facility is greatly appreciated. We thank Dr. Rhea-Beth Markowitz of Augusta University for editing the manuscript.

References:

1. Topalian SL, Drake CG, Pardoll DM. Immune checkpoint blockade: a common denominator approach to cancer therapy. Cancer Cell **2015**;27:450-61
2. Melief CJ, van Hall T, Arens R, Ossendorp F, van der Burg SH. Therapeutic cancer vaccines. J Clin Invest **2015**;125:3401-12
3. Rosenberg SA, Yang JC, Restifo NP. Cancer immunotherapy: moving beyond current vaccines. Nat Med **2004**;10:909-15
4. Overwijk WW, Theoret MR, Finkelstein SE, Surman DR, de Jong LA, Vyth-Dreese FA*, et al.* Tumor regression and autoimmunity after reversal of a functionally tolerant state of self-reactive CD8+ T cells. J Exp Med **2003**;198:569-80
5. Singh V, Ji Q, Feigenbaum L, Leighty RM, Hurwitz AA. Melanoma progression despite infiltration by in vivo-primed TRP-2-specific T cells. J Immunother **2009**;32:129-39
6. Rosenberg SA, Sherry RM, Morton KE, Scharfman WJ, Yang JC, Topalian SL*, et al.* Tumor progression can occur despite the induction of very high levels of self/tumor antigen-specific CD8+ T cells in patients with melanoma. J Immunol **2005**;175:6169-76
7. Rabinovich GA, Gabrilovich D, Sotomayor EM. Immunosuppressive strategies that are mediated by tumor cells. Annu Rev Immunol **2007**;25:267-96
8. Ahmadzadeh M, Johnson LA, Heemskerk B, Wunderlich JR, Dudley ME, White DE*, et al.* Tumor antigen-specific CD8 T cells infiltrating the tumor express high levels of PD-1 and are functionally impaired. Blood **2009**;114:1537-44
9. Zhou Q, Xiao H, Liu Y, Peng Y, Hong Y, Yagita H*, et al.* Blockade of programmed death-1 pathway rescues the effector function of tumor-infiltrating T cells and enhances the antitumor efficacy of lentivector immunization. J Immunol **2010**;185:5082-92
10. Lee PP, Yee C, Savage PA, Fong L, Brockstedt D, Weber JS*, et al.* Characterization of circulating T cells specific for tumor-associated antigens in melanoma patients. Nat Med **1999**;5:677-85
11. Dunbar PR, Smith CL, Chao D, Salio M, Shepherd D, Mirza F*, et al.* A shift in the phenotype of melan-A-specific CTL identifies melanoma patients with an active tumor-specific immune response. J Immunol **2000**;165:6644-52
12. Johnson LA, Morgan RA, Dudley ME, Cassard L, Yang JC, Hughes MS*, et al.* Gene therapy with human and mouse T-cell receptors mediates cancer regression and targets normal tissues expressing cognate antigen. Blood **2009**;114:535-46
13. Appay V, Douek DC, Price DA. CD8+ T cell efficacy in vaccination and disease. Nat Med **2008**;14:623-8
14. Aranda F, Llopiz D, Diaz-Valdes N, Riezu-Boj JI, Bezunartea J, Ruiz M*, et al.* Adjuvant combination and antigen targeting as a strategy to induce polyfunctional and high-avidity T-cell responses against poorly immunogenic tumors. Cancer Res **2011**;71:3214-24
15. Vigano S, Utzschneider DT, Perreau M, Pantaleo G, Zehn D, Harari A. Functional avidity: a measure to predict the efficacy of effector T cells? Clin Dev Immunol **2012**;2012:153863
16. Lovgren T, Baumgaertner P, Wieckowski S, Devevre E, Guillaume P, Luescher I*, et al.* Enhanced cytotoxicity and decreased CD8 dependence of human cancer-specific cytotoxic T lymphocytes after vaccination with low peptide dose. Cancer Immunol Immunother **2012**;61:817-26
17. McMahan RH, McWilliams JA, Jordan KR, Dow SW, Wilson DB, Slansky JE. Relating TCR-peptide-MHC affinity to immunogenicity for the design of tumor vaccines. J Clin Invest **2006**;116:2543-51
18. Morgan DJ, Kreuwel HT, Fleck S, Levitsky HI, Pardoll DM, Sherman LA. Activation of low avidity CTL specific for a self epitope results in tumor rejection but not autoimmunity. J Immunol **1998**;160:643-51

19. Price DA, Brenchley JM, Ruff LE, Betts MR, Hill BJ, Roederer M*, et al.* Avidity for antigen shapes clonal dominance in CD8+ T cell populations specific for persistent DNA viruses. J Exp Med **2005**;202:1349-61
20. Lichterfeld M, Yu XG, Mui SK, Williams KL, Trocha A, Brockman MA*, et al.* Selective depletion of high-avidity human immunodeficiency virus type 1 (HIV-1)-specific CD8+ T cells after early HIV-1 infection. J Virol **2007**;81:4199-214
21. He Y, Zhang J, Mi Z, Robbins P, Falo LD, Jr. Immunization with lentiviral vector-transduced dendritic cells induces strong and long-lasting T cell responses and therapeutic immunity. J Immunol **2005**;174:3808-17
22. Esslinger C, Chapatte L, Finke D, Miconnet I, Guillaume P, Levy F*, et al.* In vivo administration of a lentiviral vaccine targets DCs and induces efficient CD8(+) T cell responses. J Clin Invest **2003**;111:1673-81
23. He Y, Zhang J, Donahue C, Falo LD, Jr. Skin-derived dendritic cells induce potent CD8(+) T cell immunity in recombinant lentivector-mediated genetic immunization. Immunity **2006**;24:643-56
24. Hong Y, Peng Y, Guo ZS, Guevara-Patino J, Pang J, Butterfield LH*, et al.* Epitope-optimized alpha-fetoprotein genetic vaccines prevent carcinogen-induced murine autochthonous hepatocellular carcinoma. Hepatology **2014**;59:1448-58
25. Moran AE, Holzapfel KL, Xing Y, Cunningham NR, Maltzman JS, Punt J*, et al.* T cell receptor signal strength in Treg and iNKT cell development demonstrated by a novel fluorescent reporter mouse. J Exp Med **2011**;208:1279-89
26. Guo ZS, Naik A, O'Malley ME, Popovic P, Demarco R, Hu Y*, et al.* The enhanced tumor selectivity of an oncolytic vaccinia lacking the host range and antiapoptosis genes SPI-1 and SPI-2. Cancer Res **2005**;65:9991-8
27. Wang XL, Altman JD. Caveats in the design of MHC class I tetramer/antigen-specific T lymphocytes dissociation assays. J Immunol Methods **2003**;280:25-35
28. Mescher MF, Popescu FE, Gerner M, Hammerbeck CD, Curtsinger JM. Activation-induced non-responsiveness (anergy) limits CD8 T cell responses to tumors. Semin Cancer Biol **2007**;17:299-308
29. Gattinoni L, Klebanoff CA, Restifo NP. Paths to stemness: building the ultimate antitumour T cell. Nat Rev Cancer **2012**;12:671-84
30. Flynn JK, Gorry PR. Stem memory T cells (TSCM)-their role in cancer and HIV immunotherapies. Clin Transl Immunology **2014**;3:e20
31. Xu Y, Dotti G. Selection bias: maintaining less-differentiated T cells for adoptive immunotherapy. J Clin Invest **2016**;126:35-7
32. Guerrero AD, Welschhans RL, Chen M, Wang J. Cleavage of anti-apoptotic Bcl-2 family members after TCR stimulation contributes to the decision between T cell activation and apoptosis. J Immunol **2013**;190:168-73
33. Joshi NS, Kaech SM. Effector CD8 T cell development: a balancing act between memory cell potential and terminal differentiation. J Immunol **2008**;180:1309-15
34. Lugli E, Dominguez MH, Gattinoni L, Chattopadhyay PK, Bolton DL, Song K*, et al.* Superior T memory stem cell persistence supports long-lived T cell memory. J Clin Invest **2013**;123:594-9
35. Zhang Y, Joe G, Hexner E, Zhu J, Emerson SG. Host-reactive CD8+ memory stem cells in graft-versus-host disease. Nat Med **2005**;11:1299-305
36. Itoh Y, Hemmer B, Martin R, Germain RN. Serial TCR engagement and down-modulation by peptide:MHC molecule ligands: relationship to the quality of individual TCR signaling events. J Immunol **1999**;162:2073-80
37. Hofmann M, Radsak M, Rechtsteiner G, Wiemann K, Gunder M, Bien-Grater U*, et al.* T cell avidity determines the level of CTL activation. Eur J Immunol **2004**;34:1798-806

38. Labrecque N, Whitfield LS, Obst R, Waltzinger C, Benoist C, Mathis D. How much TCR does a T cell need? Immunity **2001**;15:71-82
39. Corse E, Gottschalk RA, Allison JP. Strength of TCR-peptide/MHC interactions and in vivo T cell responses. J Immunol **2011**;186:5039-45
40. Gattinoni L, Speiser DE, Lichterfeld M, Bonini C. T memory stem cells in health and disease. Nat Med **2017**;23:18-27
41. Fearon DT, Manders P, Wagner SD. Arrested differentiation, the self-renewing memory lymphocyte, and vaccination. Science **2001**;293:248-50
42. Gattinoni L, Zhong XS, Palmer DC, Ji Y, Hinrichs CS, Yu Z*, et al.* Wnt signaling arrests effector T cell differentiation and generates CD8+ memory stem cells. Nat Med **2009**;15:808-13
43. Gattinoni L, Lugli E, Ji Y, Pos Z, Paulos CM, Quigley MF*, et al.* A human memory T cell subset with stem cell-like properties. Nat Med **2011**;17:1290-7
44. Fuertes Marraco SA, Soneson C, Cagnon L, Gannon PO, Allard M, Abed Maillard S*, et al.* Long-lasting stem cell-like memory CD8+ T cells with a naive-like profile upon yellow fever vaccination. Sci Transl Med **2015**;7:282ra48
45. Fulton RB, Hamilton SE, Xing Y, Best JA, Goldrath AW, Hogquist KA*, et al.* The TCR's sensitivity to self peptide-MHC dictates the ability of naive CD8(+) T cells to respond to foreign antigens. Nat Immunol **2015**;16:107-17
46. Mandl JN, Monteiro JP, Vrisekoop N, Germain RN. T cell-positive selection uses self-ligand binding strength to optimize repertoire recognition of foreign antigens. Immunity **2013**;38:263-74
47. Cai Z, Kishimoto H, Brunmark A, Jackson MR, Peterson PA, Sprent J. Requirements for peptide-induced T cell receptor downregulation on naive CD8+ T cells. J Exp Med **1997**;185:641-51
48. Gallegos AM, Xiong H, Leiner IM, Susac B, Glickman MS, Pamer EG*, et al.* Control of T cell antigen reactivity via programmed TCR downregulation. Nat Immunol **2016**;17:379-86
49. Barber DL, Wherry EJ, Masopust D, Zhu B, Allison JP, Sharpe AH*, et al.* Restoring function in exhausted CD8 T cells during chronic viral infection. Nature **2006**;439:682-7
50. McMahan RH, Slansky JE. Mobilizing the low-avidity T cell repertoire to kill tumors. Semin Cancer Biol **2007**;17:317-29

Figure Legends

Fig. 1 The lv-immunized mouse splenocytes demonstrate CTL activity after AFP_{499}, but not AFP_{212}, peptide re-stimulation; and the Tet_{499}, but not Tet_{212}, cells yield antitumor effects *in vivo*. (A) The splenocytes were re-stimulated with 2μg/ml of AFP_{212} or AFP_{499} peptide in the media for 6 days before CTL assay. (B) The CTL activity of mouse splenocytes after re-stimulation with AFP_{212} or AFP_{499} was summarized from 3 mice in each group. The experiment was repeated 4 times with similar results. (C) Lvs expressing full-length opt-AFP, AFP142, and AFP164 fragments were illustrated. (D) Mice (5 in each group) immunized with indicated lv were challenged with EL4-AFP tumor cells. Tumor growth was monitored. The experiment was repeated 3 times with similar results.

Fig. 2 Tet_{212} have a lower re-activation threshold, and undergo more exhaustion and apoptosis than Tet_{499} in response to antigen re-stimulation. The beads-purified $CD45.2^+CD8^+$ T-cells were stimulated with peptide-pulsed naïve CD45.1 splenocytes or with peptide in media for 4days. (A) Representative plots of tetramer staining were presented. A summary of peptide-dose effect on Tet_{212} and Tet_{499} cell was also presented. * indicates peptides directly added to media. "0" means no re-stimulation. (B and C) The Tet_{212} and Tet_{499} cells after stimulation were analyzed for the expression of PD1 (B) and Annexin-V (C). Representative histograms and the dose-dependent induction of PD1 (B) and Annexin-V (C) (% and MFI) on Tet_{212} and Tet_{499} cells were presented. FMO: FMO: fluorescence minus one (anti-PD1 antibody) control. (D) The IFNγ production of $CD45.2^+CD8^+$ T-cells was analyzed. Representative IFNγ intracellular staining was shown. The dose response of peptide on IFNγ (% and MFI) production by Tet_{212} and Tet_{499} cells was also summarized. The % of IFNγ-producing Tet^+ were calculated by dividing the % of $IFN\gamma^+$ $CD45.2^+CD8^+$ T-cells by the % of Tet^+ cells of the same mice (Fig. 2A). (E) The inverse correlation of PD1 and IFNγ (MFI) of Tet_{212}, and the direct correlation of PD1 and IFNγ of Tet_{499}^+ cells were derived from 2B and 2D. Mean ± SE was shown. Three mice were in each group and the experiment was repeated twice with similar data.

Fig. 3 Tet_{499} undergo more expansion *in vivo* than Tet_{212} and respond to emerging tumor antigen. (A) Tet_{212} and Tet_{499} cells (5×10^5) were sorted from immunized CD45.2 mice and transferred into CD45.1 mice followed by vaccination. (B) Summarized was the kinetics of the $CD45.2^+CD8^+Tet_{212}^+$ and $CD45.2^+CD8^+Tet_{499}^+$ cells in CD45.1 mice. Three mice were in each group. The experiment was repeated twice with similar results. (C) Shown is the experimental design for studying Tet_{212} and Tet_{499} responses to vv-boost and to emerging tumor antigen AFP in autochthonous HCC model. (D) The kinetics of Tet_{212} and Tet_{499} responses in the DEN-induced mice was presented. Five mice were in each group, and the experiment was repeated twice with similar results.

Fig. 4 More Tscm is found in Tet_{499} than in Tet_{212}. (A and B) Splenocytes from the immunized mice were either directly stained (A) or were re-stimulated *in vitro* for 3 days with AFP_{212} or AFP_{499} peptide and then stained (B) for CD8, tetramer, CD44, and CD62L. Representative dot plots of Tscm, Tcm, and Teff in the Tet_{212} and Tet_{499} cells were shown. A summary data of Tcm and Tscm of 12 mice from 3 experiments are presented. (C) The Tscm of Tet_{499} cells and naive $CD44^-CD62L^+CD8^+$ cells were stained for the stem-like markers ScaI, CD122, and CCR7. Representative histograms and a summary data of 4 mice were shown. FMO: fluorescence minus one control (minus ScaI, CD122, or CCR7). The experiment was done twice with similar results.

Fig. 5 Tscm can undergo robust expansion and differentiate into Tcm and Teff *in vivo*. (A) The experimental scheme is illustrated (See Supplementary Fig.S5 for sorting strategy). Equal number (2000 cells) of the Tscm, Tcm, and Teff of $Tet499^+$ cells were transferred into CD45.1 congenic mice followed by immunization. (B) Presented were the representative dot plots of $CD45.2^+CD8^+$ and Tet_{499} cells in CD45.1 mouse blood after adoptive cell transfer. (C) The kinetics of $CD45.2^+CD8^+Tet_{499}^+$ cells after Tscm and Tcm transfer into CD45.1 mice was shown. A summary of the fold of increase of Tet_{499} after Tscm and Tscm transfer was also shown. Three mice were in each group. The experiment was repeated twice with similar results. (D) Shown is the differentiation of the $CD45.2^+$ Tscm and Tcm in CD45.1 mice. The representative plots of 3 mice were shown.

Fig. 6 The TCR signaling strength is weaker on Tet_{499} than on Tet_{212}. (A-D) The splenocytes of immunized $Nur77^{GFP}$ mice were re-stimulated 4hrs with 1μg/ml of AFP_{212} or AFP_{499} peptide in media, and GFP on the Tet_{212} and Tet_{449} cells were analyzed. (A) The representative histograms showed the GFP level on Tet_{212} and Tet_{499} cells before (open) and after (filled) re-stimulation. (B) The % and MFI of GFP^+ and $GFP^{-/lo}$ Tet_{212} and Tet_{499} cells was summarized from 3 mice. (C) A summary of dose-dependent induction of GFP^+ cells (% and MFI) was presented. (D) Histogram showed the representative CD44 staining. A summary of CD44 level on the Tet_{212} and Tet_{499} cells of 3 mice was also presented. The experiment was repeated twice with similar observations. (E and F) The beads-purified CD8 T-cells from immunized Nur^{77} mice were analyzed for GFP expression before and after stimulation with peptide-pulsed naïve CD45.1 splenocytes. (E) The representative histogram showed the basal level of GFP expression on Tet_{212} (filled) and Tet_{499} (open) prior to re-stimulation. A summary of basal GFP level from 4 mice was also presented. (F) Shown were the GFP level on $CD45.2^+CD8^+Tet_{212}$ (filled) and on $CD45.2^+CD8^+Tet_{499}$ (open) cells after 24hr stimulation with naïve CD45.1 splenocytes pulsed with indicated AFP_{212} or AFP_{499} peptides. A summary showing the dose-dependent induction of GFP (% and MFI) of 4 mice was also presented (Mean ± SE). The experiment was repeated twice with similar results.

Fig. 7 Tet_{499} TCRs have higher avidity for MHC/peptide than Tet_{212}, but their level is significantly more downregulated. (A and B) Shown was the data of tetramer binding and dissociation assays. Data shown are representative from one of 3 mice. The experiment was repeated twice with similar results. (C and D) The TCR level of Tet_{212} (C) and Tet_{499} (D) was measured. Splenocytes from the lv-vv immunized mice were stained with indicated antibodies. The $CD8^+$ and TCR $V\beta^+$ cells were analyzed for tetramer staining and CD44 and CD62L. Among the Tet^- population, $CD44^-CD62L^+$ cells were considered naïve cells, while the Tet^+ cells were considered activated T cells. The TCR Vβ level on the Tet^+ $CD8^+$ cells (red line) and Tet^- $CD44^-CD62L^+$ naïve $CD8^+$ cells (black line) were compared. (E and F) The percent of Tet_{212} and Tet_{499} TCR downregulation (E) and the absolute MFI of Tet_{212} and Tet_{499} TCR (F) were compared. Three mice were in each group. Mean ± SE was shown. (G) The kinetics of TCR

downregulation on Tet_{212} and Tet_{499} was presented. At each time point, blood T cells were analyzed for TCR downregulation as stated above. Three mice were in each group. Mean ± SE was shown at each time point. The experiment was repeated twice with similar results.

Fig.1

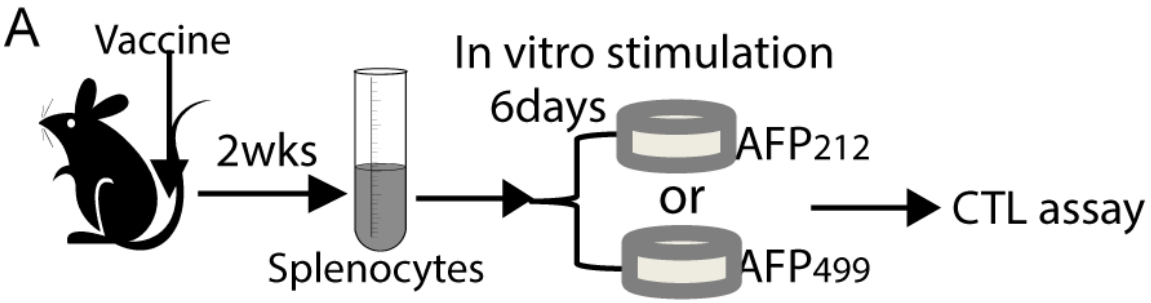
A
Vaccine
2wks
Splenocytes
In vitro stimulation
6days
AFP212
or
AFP499
CTL assay

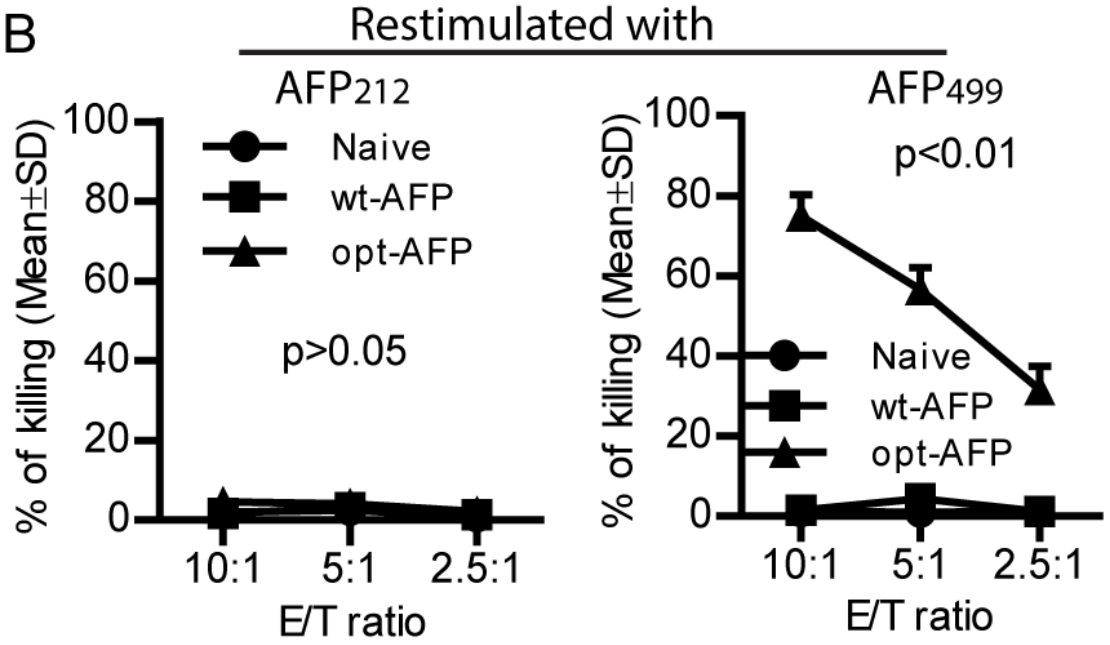
B
Restimulated with
AFP212
AFP499
Naive
wt-AFP
opt-AFP
p>0.05
p<0.01
% of killing (Mean±SD)
100
80
60
40
20
0
10:1
5:1
2.5:1
E/T ratio

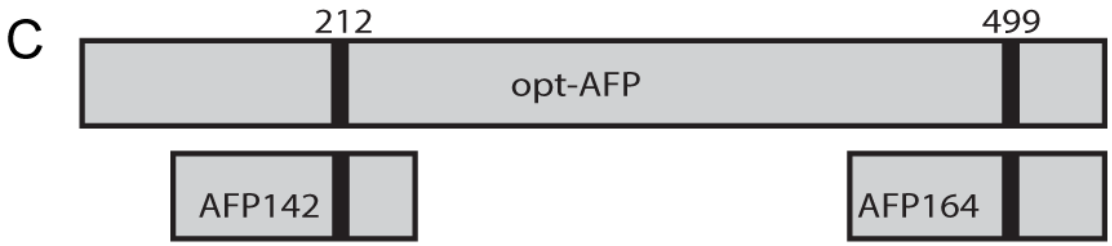
C
212
499
opt-AFP
AFP142
AFP164

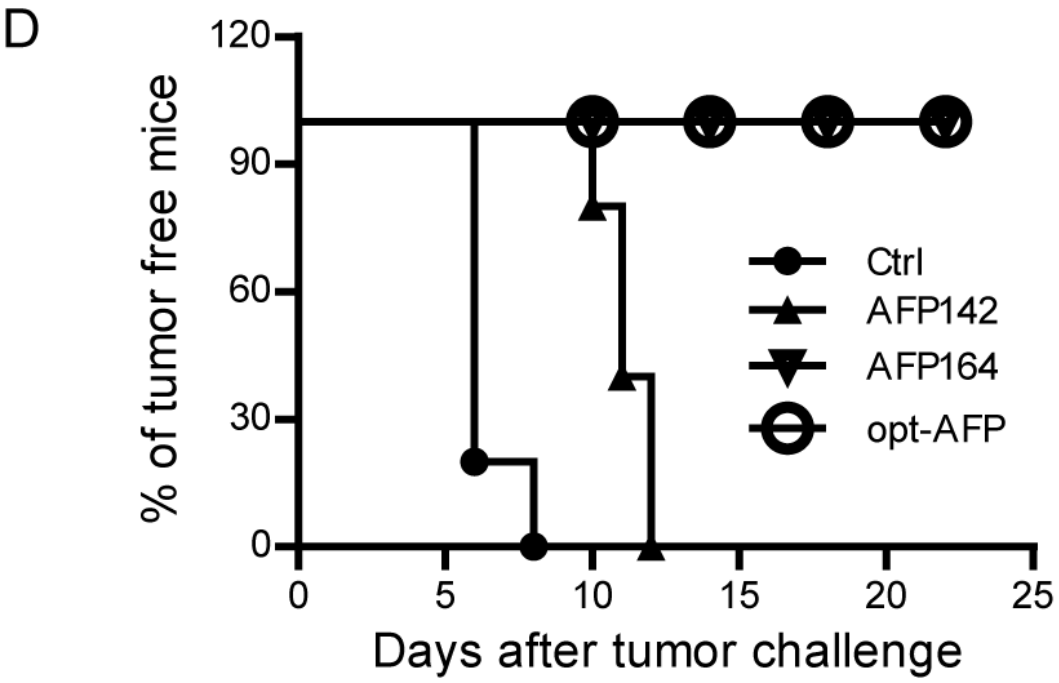
D
% of tumor free mice
120
90
60
30
0
0
5
10
15
20
25
Days after tumor challenge
Ctrl
AFP142
AFP164
opt-AFP

Fig.2

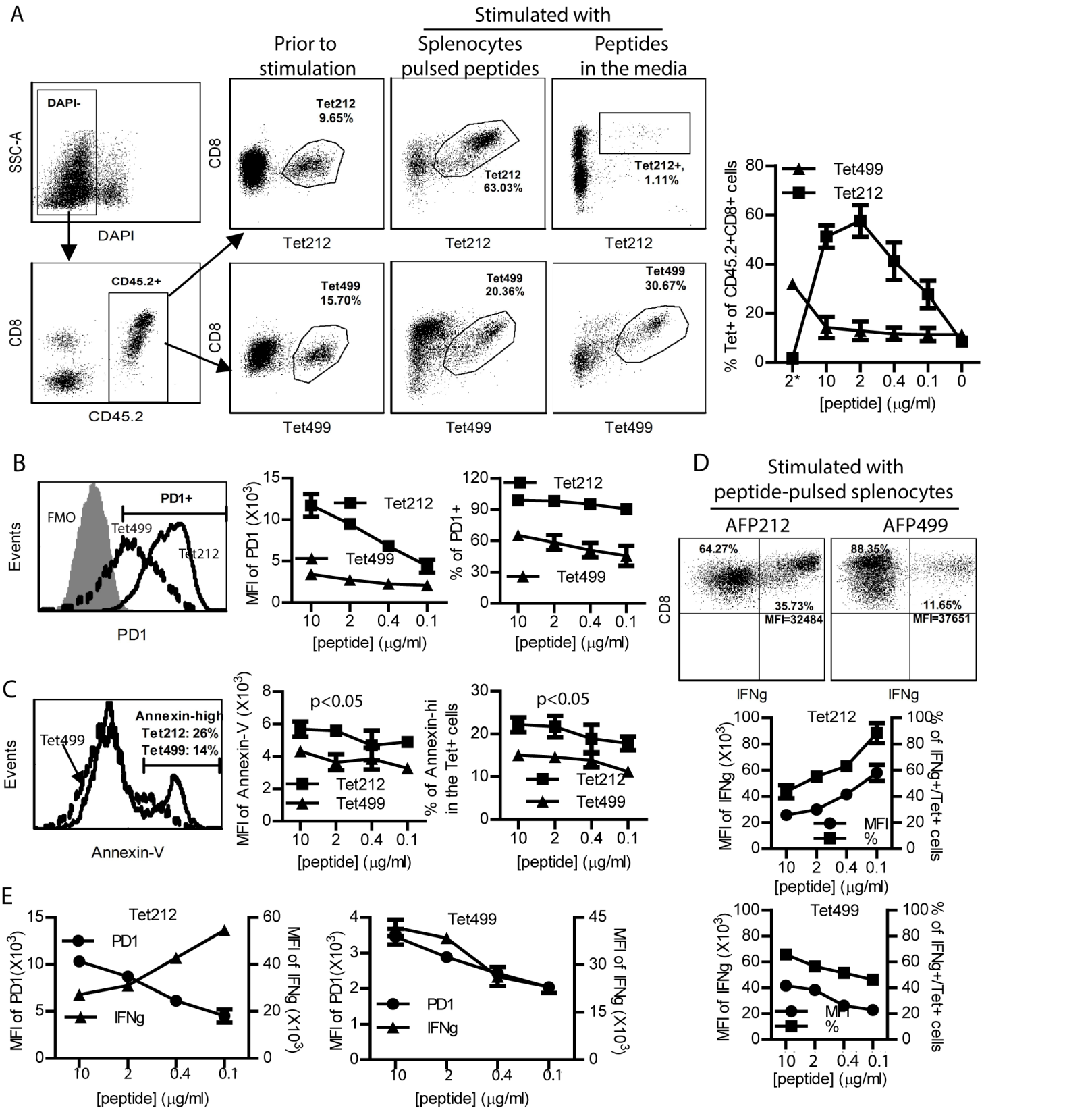
A
Stimulated with
Prior to stimulation
Splenocytes pulsed peptides
Peptides in the media
DAPI-
SSC-A
DAPI
CD45.2+
CD8
CD45.2
Tet212
9.65%
63.03%
1.11%
Tet212+,
Tet499
15.70%
20.36%
30.67%
Tet499
% Tet+ of CD45.2+CD8+ cells
[peptide] (μg/ml)
B
PD1+
FMO
Tet499
Tet212
Events
PD1
MFI of PD1 (X10³)
% of PD1+
C
Annexin-high
Tet212: 26%
Tet499: 14%
Annexin-V
MFI of Annexin-V (X10³)
p<0.05
% of Annexin-hi in the Tet+ cells
D
Stimulated with peptide-pulsed splenocytes
AFP212
AFP499
64.27%
35.73%
MFI=32484
88.35%
11.65%
MFI=37651
IFNg
MFI of IFNg (X10³)
% of IFNg+/Tet+ cells
MFI
%
E
PD1
IFNg
MFI of PD1(X10³)
MFI of IFNg (X10³)

Fig.3

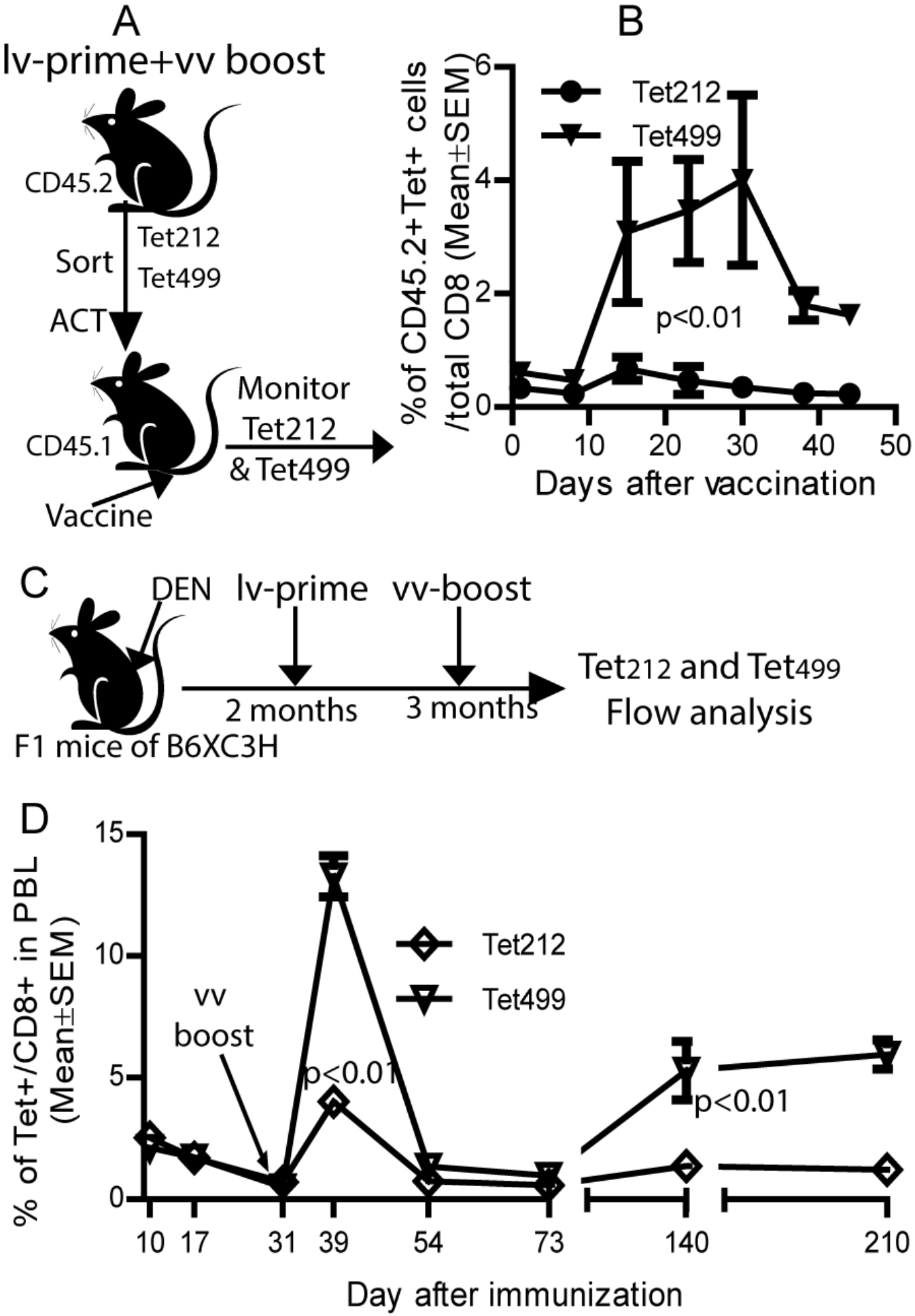
A
lv-prime+vv boost
CD45.2
Tet212
Tet499
Sort
ACT
CD45.1
Monitor
Tet212
& Tet499
Vaccine
B
% of CD45.2+Tet+ cells
/total CD8 (Mean±SEM)
Tet212
Tet499
p<0.01
Days after vaccination
C
DEN
lv-prime
vv-boost
2 months
3 months
Tet212 and Tet499
Flow analysis
F1 mice of B6XC3H
D
% of Tet+/CD8+ in PBL
(Mean±SEM)
vv
boost
Tet212
Tet499
p<0.01
p<0.01
Day after immunization

Fig.4

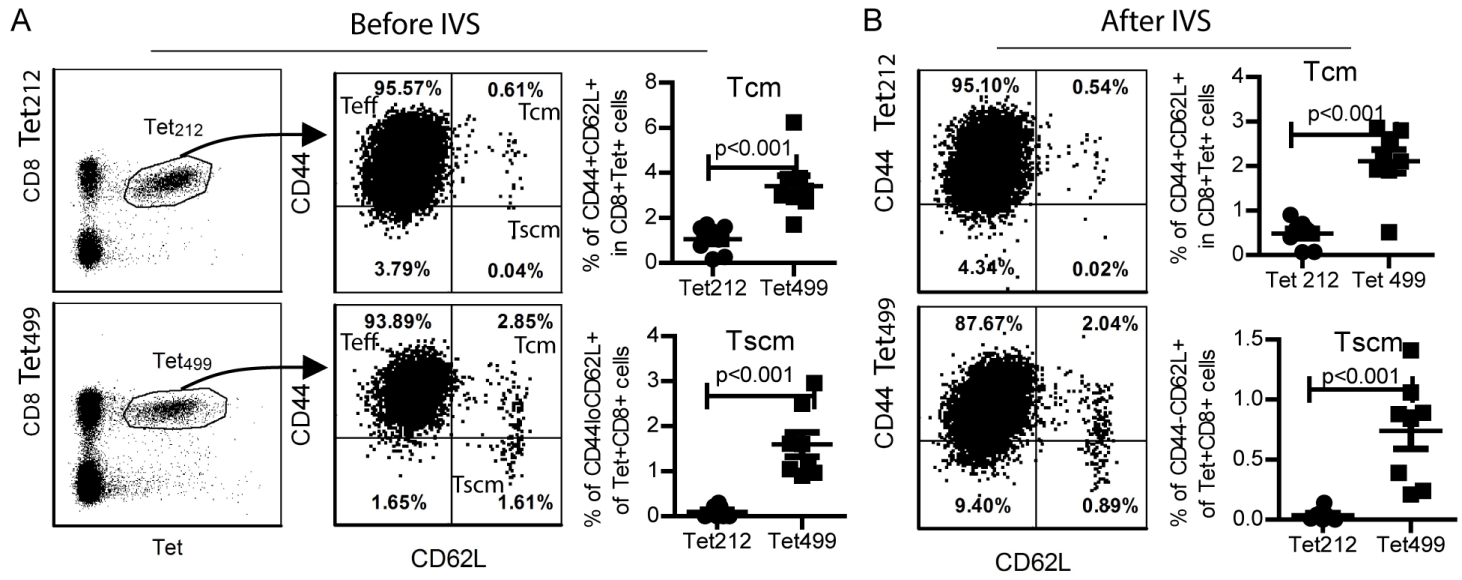
A
Before IVS
Tet212
CD8 Tet212
Tet212
CD44
95.57%
Teff
0.61%
Tcm
Tscm
3.79%
0.04%
% of CD44+CD62L+ in CD8+Tet+ cells
Tcm
p<0.001
Tet212 Tet499
CD8 Tet499
Tet499
93.89%
Teff
2.85%
Tcm
Tscm
1.65%
1.61%
% of CD44loCD62L+ of Tet+CD8+ cells
Tscm
p<0.001
Tet212 Tet499
Tet
CD62L
B
After IVS
CD44 Tet212
95.10%
0.54%
4.34%
0.02%
% of CD44+CD62L+ in CD8+Tet+ cells
Tcm
p<0.001
Tet 212 Tet 499
CD44 Tet499
87.67%
2.04%
9.40%
0.89%
% of CD44-CD62L+ of Tet+CD8+ cells
Tscm
p<0.001
Tet212 Tet499
CD62L

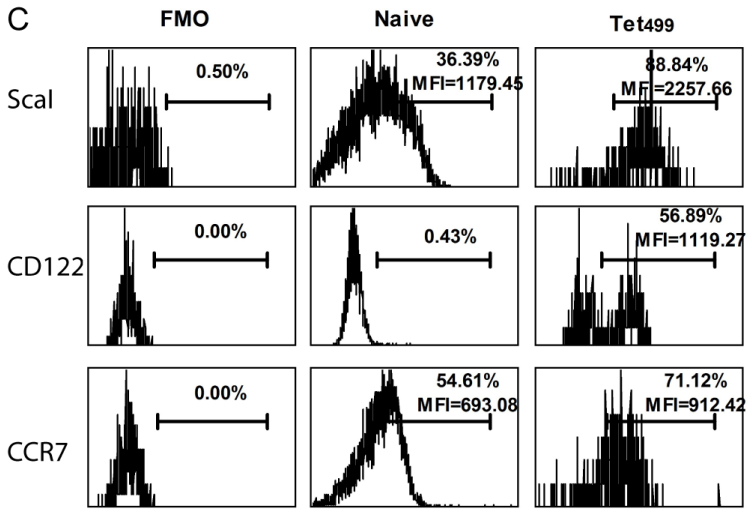
C
FMO
Naive
Tet499
Scal
0.50%
36.39%
MFI=1179.45
88.84%
MFI=2257.66
CD122
0.00%
0.43%
56.89%
MFI=1119.27
CCR7
0.00%
54.61%
MFI=693.08
71.12%
MFI=912.42

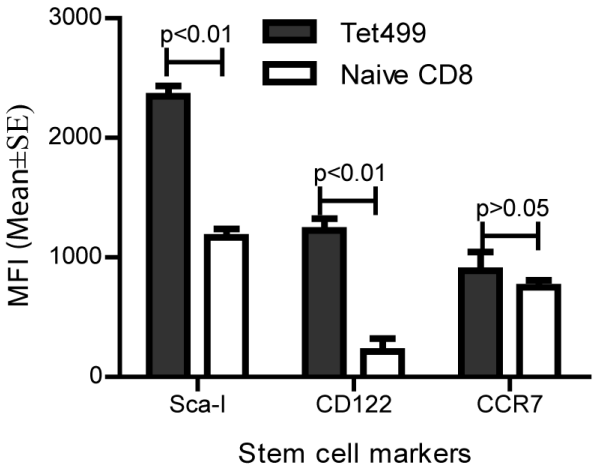
MFI (Mean±SE)
Tet499
Naive CD8
p<0.01
p<0.01
p>0.05
Sca-I
CD122
CCR7
Stem cell markers

Fig.5

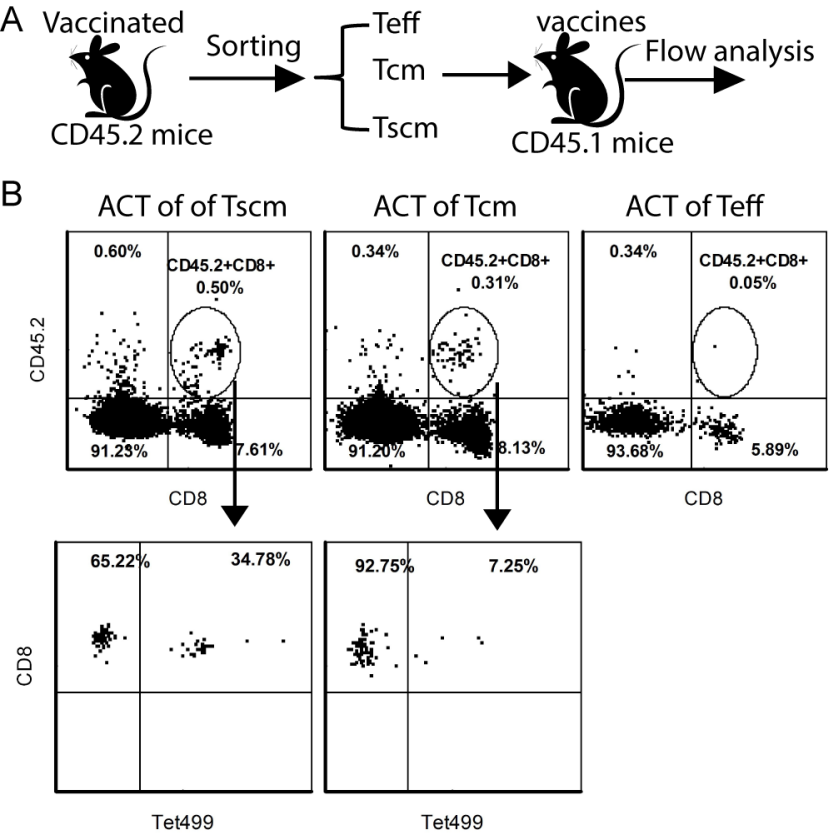
A
Vaccinated
CD45.2 mice
Sorting
Teff
Tcm
Tscm
vaccines
CD45.1 mice
Flow analysis
B
ACT of of Tscm
ACT of Tcm
ACT of Teff
0.60%
CD45.2+CD8+
0.50%
91.23%
7.61%
0.34%
CD45.2+CD8+
0.31%
91.20%
8.13%
0.34%
CD45.2+CD8+
0.05%
93.68%
5.89%
CD45.2
CD8
65.22%
34.78%
92.75%
7.25%
Tet499

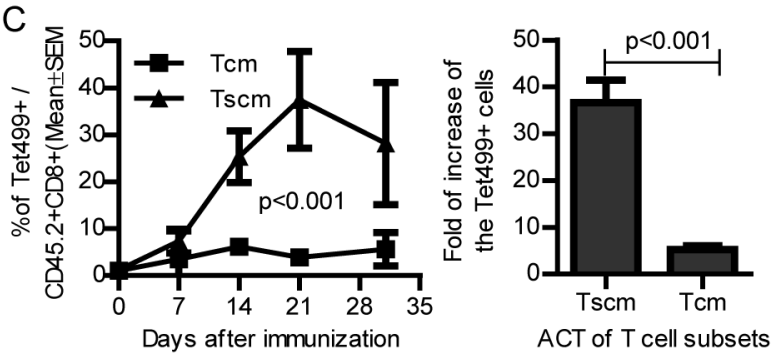
C
%of Tet499+ / CD45.2+CD8+(Mean±SEM
Tcm
Tscm
p<0.001
Days after immunization
Fold of increase of the Tet499+ cells
p<0.001
Tscm
Tcm
ACT of T cell subsets

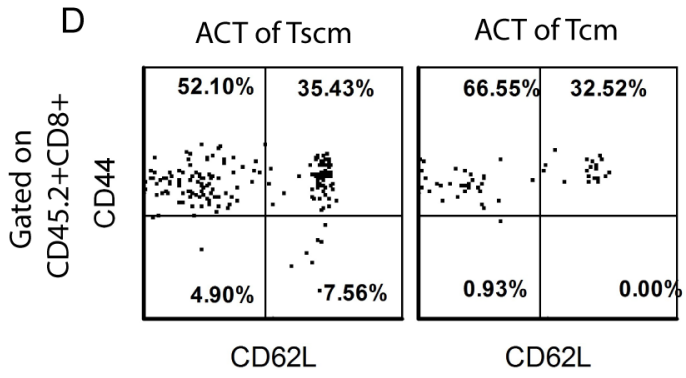
D
ACT of Tscm
ACT of Tcm
Gated on CD45.2+CD8+
CD44
52.10%
35.43%
4.90%
7.56%
66.55%
32.52%
0.93%
0.00%
CD62L
CD62L

Fig.6

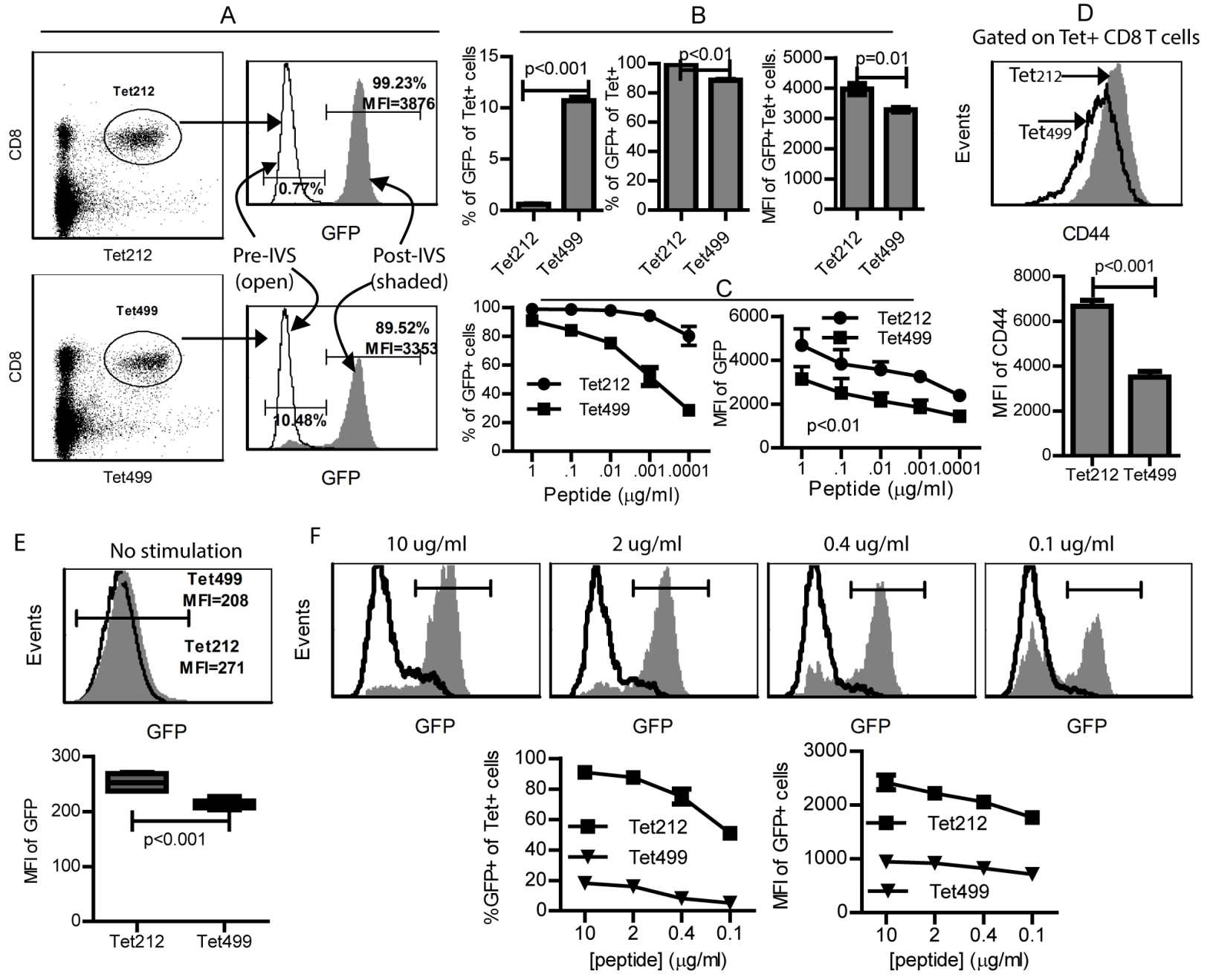
A
B
C
D
Tet212
CD8
99.23%
MFI=3876
0.77%
GFP
Pre-IVS
(open)
Post-IVS
(shaded)
Tet499
89.52%
MFI=3353
10.48%
% of GFP- of Tet+ cells
p<0.001
% of GFP+ of Tet+
p<0.01
MFI of GFP+Tet+ cells.
p=0.01
% of GFP+ cells
MFI of GFP
p<0.01
Peptide (μg/ml)
Gated on Tet+ CD8 T cells
Events
CD44
MFI of CD44
p<0.001
E
No stimulation
Tet499
MFI=208
Tet212
MFI=271
MFI of GFP
p<0.001
F
10 ug/ml
2 ug/ml
0.4 ug/ml
0.1 ug/ml
%GFP+ of Tet+ cells
[peptide] (μg/ml)
MFI of GFP+ cells

Fig.7

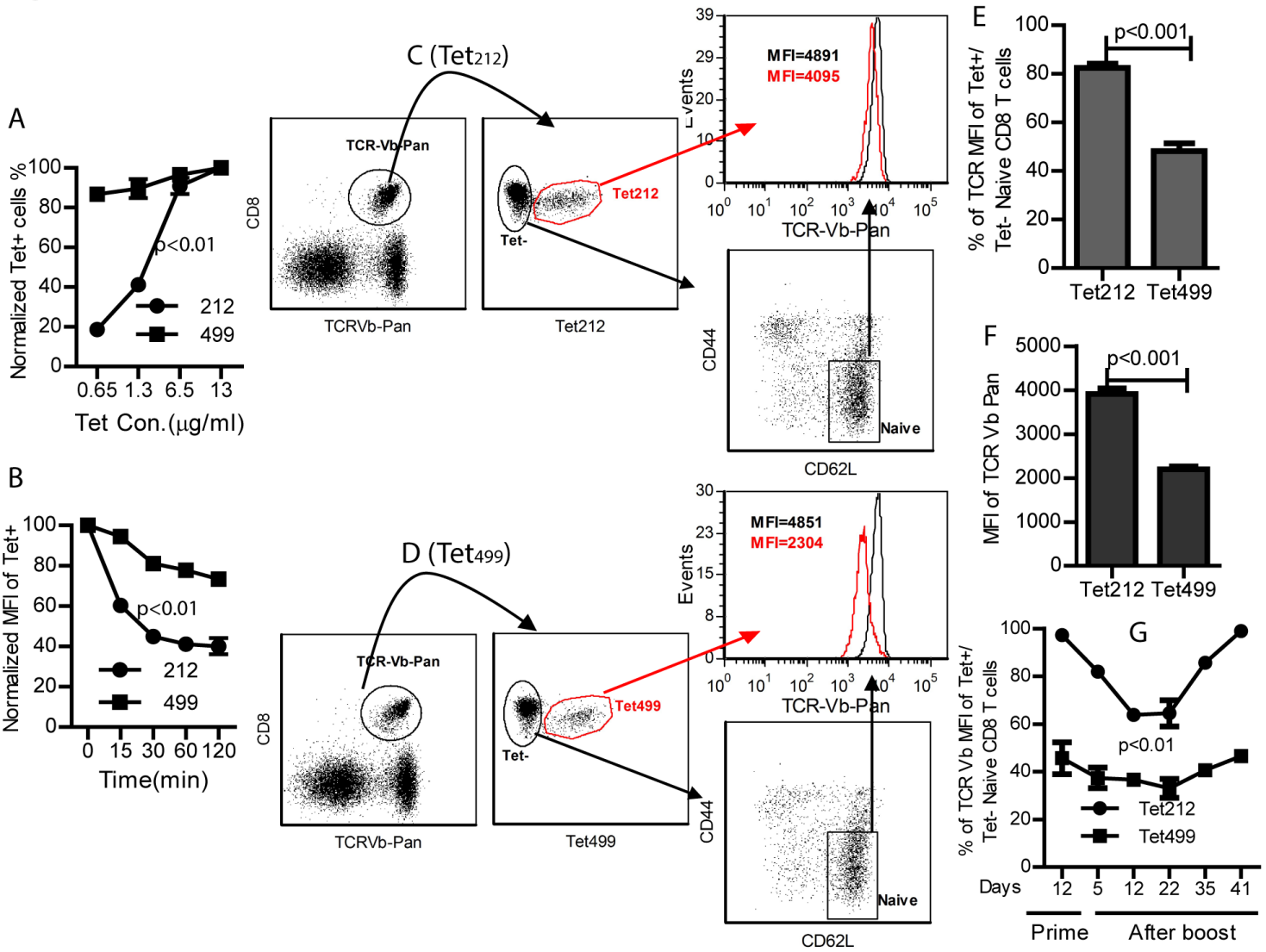
A
Normalized Tet+ cells %
p<0.01
212
499
0.65 1.3 6.5 13
Tet Con.(μg/ml)
B
Normalized MFI of Tet+
p<0.01
212
499
0 15 30 60 120
Time(min)
C (Tet212)
TCR-Vb-Pan
CD8
TCRVb-Pan
Tet212
Tet-
Events
MFI=4891
MFI=4095
TCR-Vb-Pan
CD44
Naive
CD62L
D (Tet499)
TCR-Vb-Pan
CD8
TCRVb-Pan
Tet499
Tet-
Events
MFI=4851
MFI=2304
TCR-Vb-Pan
CD44
Naive
CD62L
E
% of TCR MFI of Tet+/ Tet- Naive CD8 T cells
p<0.001
Tet212 Tet499
F
MFI of TCR Vb Pan
p<0.001
Tet212 Tet499
G
% of TCR Vb MFI of Tet+/ Tet- Naive CD8 T cells
p<0.01
Tet212
Tet499
Days
12 5 12 22 35 41
Prime
After boost